Journal of the Serbian Chemical Society
JSCS-info@shd.org.rs • www.shd.org.rs/JSCS
J. Serb. Chem. Soc. 85 (11) 1429–1444 (2020)
JSCS–5385
UDC 544.362:546.56+547.78:577.1:537872.000.57
Original scientific paper

Catalytic center of cytochrome c oxidase: Effects of protein environment on the pK_a values of Cu_B histidine ligands

DRAGAN M. POPOVIĆ* and IVANA S. ĐORĐEVIĆ

University of Belgrade – Institute of Chemistry, Technology and Metallurgy, Department of Chemistry – National Institute of the Republic of Serbia, Njegoševa 12, 11000 Belgrade, Serbia

(Received 20 July, revised 15 August, accepted 20 August 2020)

Abstract: The molecular mechanism by which electron transfer (ET) is coupled to proton pumping in cytochrome oxidase is one of the main unsolved problems in biochemistry. Particularly, the nature and position of the proton-loading site is under dispute. The Cu_B complex has three ligated histidines, whereas only His290 and His291 are ionizable sites with the same pK_a values in aqueous solution, but apparently quite different ones within the enzyme. Earlier, a model of proton pumping with the central role of His290 was proposed. Recent calculations indicate that the His291 ligand of the Cu_B center might play the role of the pumping element, since its protonation state depends on the oxidation state of the binuclear complex (BNC). The present electrostatic study was applied to assess the role of the protein environment on the acidity of the two histidines. Their pK_a values and effects of different energy terms were evaluated to discover the nature of their diverse behavior in the enzyme. Here, a new set of pK_a values for the non-standard model compounds within the BNC was applied. The enhanced results are compared with results of previous studies in the light of the plausible proton pumping mechanism. The obtained microscopic and apparent pK_a values in the oxidized state of BNC are virtually the same, indicating that deprotonated form of His291 accounts for the large pK_a increase of His290, since then both titratable sites on then Cu_B center cannot simultaneously be in the charged state. The present results support the underlined His291 pumping model.

Keywords: Bioenergetics; binuclear complex; bovine; histidine ligands; linear Poisson–Boltzmann equation; pK_a calculations; reaction and protein field.

INTRODUCTION

Cytochrome c oxidase (CcO), the terminal membrane-bound enzyme of the respiratory electron transport chain, is responsible for processing most of the biological oxygen and generating in part the proton gradient used in the synthesis

* Corresponding author. E-mail: dpopovic@chem.bg.ac.rs
https://doi.org/10.2298/JSC200720047P

of ATP in aerobic cells.[1] The energy released from the reduction of molecular oxygen to water in the binuclear complex (BNC), the active site of the enzyme, is used to pump protons across the bacterial periplasmic or the inner-mitochondrial membrane against the electrochemical proton gradient in aerobic bacteria and animal cells. Thus, it could be stated that oxygen in the BNC is the ultimate sink for the electrons from the respiratory electron transport chain. In the process, protons are pumped across the membrane and oxygen is reduced to form water.[2]

CcO contains four redox-active metal centers: Cu_A, heme *a* (Fe_a), and the BNC consisting of heme a_3 (Fe_{a3}) and Cu_B. In the intricate catalytic cycle, electrons are successively transferred through the metal centers to the active site (BNC), where reduction of oxygen occurs.[3] To be split, a molecule of O_2 bound to the reduced form of BNC requires four electrons. Two electrons are provided by Fe^{2+}, one electron by Cu^{1+} and the fourth electron and a proton are supplied by Tyr244, which turns into the Tyr• neutral radical state. Once this is attained, only different forms of oxygen intermediates remain present in the BNC (*e.g.*, =O, HO^-, H_2O). The transfer of each electron required for the reduction of oxygen intermediates is accompanied by the translocation of two protons, one of which is consumed internally in the binuclear center for the chemical reduction of substrate species (chemical/substrate proton) and the other is pumped across the membrane (pumped proton). The overall reaction catalyzed by CcO can be expressed as follows:

$$O_2 + 4e^- + 8H^+_{(N)} \rightarrow 2H_2O + 4H^+_{(P)}$$

where (N) and (P) indicate two sides of the mitochondrial membrane: the inner (negatively charged) matrix side and the outer (positively charged) intermembrane space, respectively. The chemical and pumped protons are provided along the entrance proton-conducting D- and K-channels, whereas the majority of 6–7 protons are delivered along the D-channel, which provides all four pumped protons.[4] Presumably, the Glu242 residue is the major proton donor in the enzyme, while Lys319 plays a role in the reductive half of the catalytic cycle providing only 1–2 chemical protons.[5,6]

In the past decades, the structure of CcO has been solved for several organisms.[4,7–10] However, details of the molecular mechanism of proton pumping still remain a subject of intense debate. In particular, the identity of the proton-pumping site, the key element of the mechanism, is unknown. A number of models have been proposed,[9–19] however, there is no agreement on the major issues, such as the location of the pumping site and how it pumps protons. Beyond doubt, this is also an incredibly difficult experimental task, since the measurements of the kinetics of proton translocation cannot uniquely pin point a single residue as the pumping site.[19,20] Similar problems are encountered with all other advanced experimental techniques due to the close proximity and strong

coupling of all potential PLS. Recent reviews of the enzyme structure, function and kinetics can be found in the literature.[1,3,6,17,20–27]

In order to determine the mechanism of proton pumping in CcO, a number of the Poisson–Boltzmann (PB) based continuum electrostatic[14,28,29] and combined DFT/electrostatic calculations[30–32] have recently been performed on the redox-dependence of the protonation state (*i.e.*, calculation of the protonation energies and pK_a values) of CcO. These calculations point to a possible key role played by His291, one of the ligands to the Cu_B center of the enzyme, which seems to change the protonation state depending on the redox state of the Fe_{a3} and Cu_B centers. These results suggest a possible mechanism for proton pumping in CcO.[28] On the other hand, an earlier proposal suggested the His290 ligand as a possible pumping site, which is deprotonated in the oxidized state of the binuclear complex.[12]

Proton pumping mechanism in CcO

The proposed proton pumping mechanism based on the Coulomb pump model with kinetic gating[28] is shown schematically in Fig. 1. The steady state during the catalytic cycle is established when a chemical proton is accepted by one of the hydroxy ligands of the BNC. In the steady state of the catalytic center, one of the metal centers is formally oxidized (Fe^{3+}–H_2O or Cu^{2+}–H_2O), while Glu242 is protonated and His291 (Nδ1 site) is deprotonated. In order to proceed further, the enzyme needs an additional electron to be supplied to the system by cyt c to the Cu_A center and transferred further to heme *a* (step 1), and then to the heme a_3–Cu_B binuclear center (step 2). In response to the increase of negative charge of the BNC, the proton from Glu242 has now a driving force to move closer to the catalytic center. There are two proton-conducting pathways leading from Glu242 to two possible sites: one is leading to the OH^- group in the BNC, the second is leading to the deprotonated His291 site (PLS). Both groups show a high proton affinity, which is revealed by their high pK_a values.[14,31] Since the proton translocation rate to His291 is considerably larger than the one to OH^- group,[19,20] in the next step, protonation of His291 occurs, *i.e.*, transfer of a pump proton to the PLS. Thus, the kinetics (not thermodynamics) control this proton transfer (PT) reaction resulting in the formation of a meta-stable state of the enzyme[28,29] in step 3. Step 4 is the reprotonation of the Glu242 residue through the D-channel by proton uptake from the N-side of the membrane. Now the second chemical proton, using a separate water chain path, can be transferred to the BNC protonating OH^- to H_2O (step 5). The presence of an additional positive charge in the BNC consequently decreases the pK_a value of His291.[30,31] Obviously, the entrance of a substrate proton into the active site is an essential component of the pumping mechanism in CcO, since the free energy is generated at the catalytic center. In step 6, Glu242 presumably the main proton donor of the

proton translocation process, once again becomes reprotonated through the D-channel. This additionally increases the electrostatic repulsion between a proton at His291 and the H_2O ligand in the BNC, which finally, in step 7, leads to expulsion of a preloaded proton from the PLS to the P-side of the membrane.[33] Therefore, reprotonation of the proton donor site may control a proton release from the PLS to the P-side of the membrane, additionally facilitating the proton pumping event.[23,33] Moreover, the reprotonation of Glu242 along with the release of the pumped proton controls entry of the next electron into the enzyme, since the reduction of heme *a* is only feasible if Glu242 is in the protonated steady state.[32] Such control of the flow of electrons assures that electrons are taken up and consumed one at a time in the active site of the enzyme.

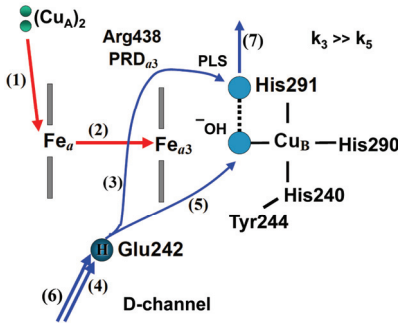

Fig. 1. The sequence of steps in the proton pumping mechanism of CcO. Red and blue arrows display the ET and PT steps, respectively. Glu242 is connected to His291 (PLS) and OH^- ligand in the active site (BNC) by two separate proton-conducting water chains with different proton-conducting rates (k_3>>k_5). The faster chain delivers the pumped protons to PLS, whereas the slower chain delivers the chemical protons to BNC. The difference in the rates ensures that a proton is preloaded into the pump site (PLS) before protonation of the reduced oxygen intermediate by the chemical proton occurs.[19,20,28]

The OH^- group can be bound to Cu_B or Fe-a_3 metal ion depending on the transition state in the catalytic cycle. In both cases, the entrance of the chemical proton would form a H_2O molecule in the BNC. A H_2O ligand in the BNC causes repulsive interactions with the proton on the PLS in the oxidized state of the BNC. As a consequence, a release of the pumped proton from the PLS, *i.e.*, a pumping event, occurs.

The scheme shown in Fig. 1 repeats with each new electron entering the system. Since four electrons are required for complete reduction of O_2 to $2H_2O$, the displayed sequence of steps repeats four times to complete a full catalytic cycle of the enzyme. The proposed sequence of steps also ensures the stoichiometry of one pumped H^+ per one e^- passed through the system. For details of the catalytic cycle of CcO, the reader is referred, for example, to the literature[22,28] dedicated to the topic of the transition states (A-, P_m-, P_r-, F-, H-, O-, E-, R-state) and the corresponding changes in the BNC during the catalytic cycle.

The ET to the BNC is coupled with the fast PT to the PLS (k_3), while the following slow PT of a chemical proton into BNC (k_5) is accompanied by expulsion of the pre-loaded proton from the PLS. The difference in the proton conducting rates, k_3>>k_5, was initially a pre-request of the proposed pumping model

in order to work and pump protons.[14,28] Otherwise, the supplied protons would go to the BNC for chemical reduction of oxygen species and the formation of H_2O molecules without pumping. This indeed happens with certain mutations, which significantly disturb the proton-conducting water chains and therefore, change the ratio of the corresponding k_3 and k_5 rates.[6] Later on, the proposed kinetic gating model obtained the experimental support by time-resolved electrometric measurements of the membrane potential generated by CcO inserted in vesicules[20] and by studies of the deuterium kinetic isotope effects.[23]

One focus of this work was to study the interactions of the protein environment with the Cu_B center and its histidine ligands in bovine cytochrome *c* oxidase. The magnitude of the effects in terms of the reaction and protein field on the pK_a values of the two histidine ligands, His290 and His291, of Cu_B center were estimated. The other goal was to implement a new enhanced set of pK_as for non-standard model compounds obtained by DFT/solvation electrostatic calculations and to compare the present results with the results of a previous study[14] in the light of the possible proton-loading site and the proton pumping mechanism in CcO inserted into membrane.

The structure of the paper is as follows. In the next section, a basic description is given of how to solve the linear Poisson–Boltzmann equation (LPBE) numerically on a grid for a protein in inhomogeneous dielectric medium by using a continuum electrostatic model for the solvent, and how from there to evaluate the protonation energies and pK_a values of titratable groups in CcO. In the results section, by using additivity of the solutions of the LPBE, it was possible to separate the different energy contributions and to discuss their effects on the acidity of the Cu_B histidine ligands in light of the possible proton-loading site in the pumping mechanism of CcO. Moreover, new improved pK_a values of the model compounds in aqueous solution, which were calculated by the DFT/electrostatic method, were used. In last section, the results of the paper are summarized.

EXPERIMENTAL

Continuum electrostatic pK_a calculations

The electrostatic calculations have been performed by using program suite MEAD,[34,35] as described and reviewed in detail elsewhere.[34,36-43] Here we briefly summarize the approach and describe the modifications employed in our calculations.

The protonation state of titratable groups in CcO are determined simultaneously by averaging over all protonation states of the titratable groups for the given redox state of the metal centers. To obtain the electrostatic energies of the different protonation states, the linear Poisson–Boltzmann equation (LPBE) is solved for the appropriate molecular systems:

$$\nabla\left[\varepsilon(\vec{r})\,\nabla\phi(\vec{r})\right] = -4\pi\rho(\vec{r}) + \kappa^2(\vec{r})\phi(\vec{r}) \quad (1)$$

The charge distribution $\rho(r)$ is derived from the atomic partial charges of a given molecular system. The ionic strength is defined through the parameter κ, the inverse Debye length.

Dielectric constant of 80 is used for the solvent and 4 within the protein to obtain the electrostatic potential $\phi(\boldsymbol{r})$; for a full discussion on the choice of dielectric constants, see literature.[42]

Protonation and redox states of the individual ionizable groups depend on each other. The protonation probability $\langle x_\mu \rangle$ of a titratable group μ can be expressed by the total Boltzmann sum as a thermodynamic average over all 2^N possible charge patterns of the N ionizable groups of the molecular system according to:

$$\left\langle x_\mu \right\rangle = \frac{1}{Z}\sum_{n=1}^{2^N} x_\mu^{(n)} \exp\left(\frac{G^{(n)}}{RT}\right) \quad \text{with} \quad Z=\sum_{n=1}^{2^N}\exp\left(\frac{G^{(n)}}{RT}\right) \tag{2}$$

where T is the absolute temperature and R the universal gas constant. The charge state of group μ for the charge pattern (n) is characterized by the integer $x_\mu^{(n)}$, which adopts the value of 0 or 1 depending on whether group μ is deprotonated or protonated.

The free energy $G(\vec{\mathbf{n}})$ of a specific protonation state of the enzyme $(\vec{\mathbf{n}})$ is given as:

$$G(\vec{\mathbf{n}}) = \sum_{\mu=1}^{N} x_\mu^{(n)} RT \ln 10\left(pH - pK_{a,\mu}^{intr}\right) + \frac{1}{2}\sum_{\mu=1}^{N}\sum_{\nu=1}^{N} x_\mu^{(n)} x_\nu^{(n)} W_{\mu\nu} \tag{3}$$

where **n** is the N-dimensional protonation state vector. The first sum runs over all N protonable sites and the second term is associated with the charge–charge interactions between all N ionizable groups in the system. The intrinsic pK_a is defined as pK_a of the site μ in protein when all other sites are in their neutral state, so-called the reference state.[34]

The total free energy G(**n**) of the charge pattern (**n**) of the considered molecular system can be further simplified and expressed as:

$$G(\vec{\mathbf{n}}) = \sum_{\mu=1}^{N}\left[x_\mu^{(n)} \Delta G_\mu^{intr} + \frac{1}{2}\sum_{\nu=1}^{N} x_\mu^{(n)} x_\nu^{(n)} W_{\mu\nu} \right]. \tag{4}$$

The mutual interaction energies $W_{\mu\nu}$ of the titratable groups, μ and ν, refer to their charge pattern, where all other ionizable groups of the molecular system are in the neutral reference state. The strength of the electrostatic coupling between the two titratable groups, μ and ν, is expressed by the $W_{\mu\nu}$ matrix elements. The intrinsic free energy, ΔG_μ^{intr} accounts for the three addition energy terms:

$$\Delta G_\mu^{\text{intr}}\ (\text{pH}) = RT\ln 10\left(\text{pH} - pK_{a,\mu}^{\text{model}}\right) + \left(\Delta G_{\text{Born},\mu}^{\text{protein}} - \Delta G_{\text{Born},\mu}^{\text{model}}\right) + \left(\Delta G_{\text{back},\mu}^{\text{protein}} - \Delta G_{\text{back},\mu}^{\text{model}}\right) \tag{5}$$

The first term in Eq. (5) accounts for the electrostatic free energy of the corresponding titratable group μ, which is used as model compound in aqueous solution with known pK_a value. For amino acids, the experimental values of the model compounds in aqueous solution can be found elsewhere.[44] The second term, the Born energy (desolvation penalty), accounts for the difference in self-energy to protonate the titratable group μ in the protein and in aqueous solution. The last term provides the corresponding energy difference resulting from the interactions of group μ with the background charges, *i.e.*, the charges of non-titratable residues and the charges of all other titratable sites in their uncharged reference state. For a detailed description of these energy terms.[35,39] The free energy G(**n**), Eq. (4), of the protonation pattern (**n**) of the considered molecular system is determined by calculating the electrostatic energies from the solution of the LPBE by using program MULTIFLEX.[34,35]

Having the electrostatic energy G(**n**) for each configuration (**n**) and using Eq. (1), one can compute the average protonation state of all titratable groups in the protein and evaluate

their pH dependence. The exact summation over all 2^N configurations, however, for a protein containing over 100 titratable sites is not feasible. Therefore, to evaluate $\langle x_\mu \rangle$, the Monte Carlo (MC) method has been employed.

Definition of the pK_a *of protonable groups in a protein environment*

The free energy difference between the charged and uncharged state of the protonable group μ depending on pH value and redox potential of the solvent E_{sol} is defined in terms of the ratio of probabilities that this group is protonated or deprotonated according to:

$$\Delta G_\mu(\mathrm{pH}, E_{sol}) = -RT \ln \frac{\langle x_\mu \rangle}{1 - \langle x_\mu \rangle} \tag{6}$$

With this free energy difference, the pK_a value of a titratable group μ in the protein environment can be written as:

$$\mathrm{p}K_{a,\mu}^{\mathrm{protein}}(\mathrm{pH}, E_{sol}) = \mathrm{pH} - \frac{\Delta G_\mu(\mathrm{pH}, E_{sol})}{RT \ln 10} \tag{7}$$

The pK_a of a protonable group at pH 7 ($pK_{a,7}$) is calculated simultaneously on the self--consistent way, as the thermodynamic average over the charge states of all ionizable groups of cytochrome *c* oxidase for a given redox state of the metal centers, as explained in detail elsewhere.[16,44]

Computational model

The electrostatic calculations are done on the two subunits *A* and *B* of the crystal structure of mitochondrial cytochrome *c* oxidase from bovine heart at the fully oxidized state (PDB code: 1V54) obtained at a resolution of 1.9 Å, solved by Yoshikawa and coworkers, 2003.[9] The method is based on solving the LPBE for a model of protein in aqueous solution, thus for the inhomogeneous dielectric system. A usage of membrane is easy to implement for the trans-membrane protein complexes, while further generalization is possible for any other solvent, and any number of variably charged states of titratable group μ. We used the simple model of protein–solvent–membrane system defined with the standard dielectric parameters: $\varepsilon_{protein} = \varepsilon_{membrane} = 4$, $\varepsilon_{solvent} = \varepsilon_{cavity} = 80$ to calculate protonation pattern of bovine CcO in the OORO and OORR redox states. The letters O and R designate a formally oxidized or reduced state of each redox center in CcO: Cu_A, heme *a*, heme a_3 and Cu_B, respectively. The two last letters specify the redox state of BNC, whereas the BNC in OORR state is reduced in respect to the OORO state of CcO, see, *e.g.*, refs.[13,14] For preparation of the structure, a list of used atomic charges, and all other computational details, we refer a reader to refs.[14,33,45]

The protein charges and atomic radii that we use in this application have been successfully used before to calculate the pK_a values of protonable groups, redox potentials of cofactors and bioenergetics of ET and PT reactions in different enzymes and proteins.[14,25,29,32,33,44,46,47]

RESULTS AND DISCUSSION

Local dielectric and protein environment around His-ligands

Protein environment around the two His is displayed in Fig. 2 striking the mutual differences. His290 is located in a relatively small cavity and engaged in the hydrogen-bonding network with Thr309 and Phe305 anchoring and stabilizing the Cu_B center to the protein matrix. The titratable proton on Nδ1 of His290 is a proton donor in a H-bond[9] and can, in principle, deprotonate and move to

Oγ1 of Thr305, which would then move its own proton to the C=O backbone of Phe305. From there a feasible exit for the proton most likely leads to Asp364 and PRA of heme a_3. A possible problem here could make the very strong coupling between Asp364 and PRAa_3 (810 meV, *i.e.*, 13.6 p*K*-units), which are H-bonded and already share one proton in both the OORO and OORR redox states. In addition, PRAa_3 is strongly H-bonded to His368, the ligand of the redox-inactive Mg^{2+}-center and to the water molecule w1, at least in some redox and transient states of CcO. His290 site was earlier proposed as the central player in the structural model of proton pumping.[12] The proposed path of proton translocation from His290 includes two steps, first PT to the Asp364–PRAa_3 pair and then PT to the Arg438/Arg439–propionate region around heme a_3 and heme *a*.

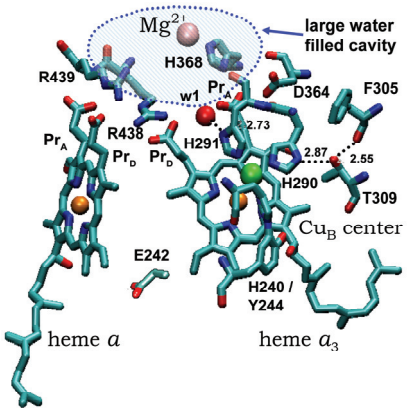

Fig. 2. The center part of the bovine CcO structure reveals the different dielectric and local protein environment around the two histidine ligands (His290 and His291) of the Cu_B metal center.

On the other hand, His291 is widely open to the hydrophilic (water filled) cavity on the interface between the two subunits *A* and *B* that is located above the heme propionates. His291 is surrounded by many polar, titratable and charged residues, and hydrogen-bonded to a water molecule (w1) sitting in the interspace between the propionates of heme a_3 and histidine (Nδ1 atom). This water molecule is visible in all crystal structures[4,7–10] and is a part of the H-bond network that involves a dozen of water molecules and polar/charged residues, including PRAa_3 and PRDa_3. His291 is just in the right position to deprotonate (in the oxidized state of the BNC) and to release a H^+ along a putative proton exit pathway.[29]

Protonation energies and microscopic pK_a values of the histidine ligands

First, the protonation energies and microscopic pK_a values of the two histidines, His290 and His291, which are part of Cu_B complex, were examined. The calculations were performed at room temperature $T = 298$ K and the physiological pH 7, *i.e.*, at the conditions of the catalytic activity of CcO. The Cu_B center is ligated by three imidazoles of His240, His290 and His291, whereas the

fourth coordination place is reserved for oxygen intermediates, *i.e.*, OH^- or H_2O. In fact, only His290 and His291 are ionizable sites, since His240 is covalently connected (cross-linked) to Tyr244 by a post-translational modification between Nδ1 and the Cε1 atom, respectively. However, Tyr244 is also an independent protonable group in the present calculations. The quantum-mechanical computations in SCRF with $\varepsilon = 80$ (aqueous phase) showed that the two histidines are equal with the same pK_a value of 8.9 and 14.4, for the oxidized (Cu_B^{2+}) and reduced (Cu_B^{1+}) metal center, respectively.[31,45]

His290 and His291 are strongly coupled sites belonging to the same molecular group, since they both use Nε2 atoms to become directly coordinated to Cu_B metal center. Their energy of coupling is around 520 meV, *i.e.*, 8.7 p*K*-units. (the situation is similar as for a non-coordinated His residue with strongly coupled titratable sites on Nδ1 and Nε2 atoms, where both sites could be protonated or only one of them, but deprotonation of both N-sites never occurs over the whole pH 0–14 range). Technically within PB electrostatic calculations, there are several ways to calculate the microscopic pK_a values of His290 and His291 sites within the Cu_B center in CcO. They could be considered as independent titratable groups. Then to apply a high bias energy to keep one of the residues in the fixed protonated or deprotonated state and to calculate the protonation energy and p$K_{a,7}$ of the other site. Implementation of the "super residue" titratable groups[44] consisting of the coordinates and charges of the two histidines is also feasible. Then again, the charges for the fixed His site will be the same in both variably charged states and different (protonated/deprotonated) for the other His. Finally, it is possible that all the above-mentioned modifications are directly implemented in the CcO.pqr file itself and to repeat the calculations 4 times. The obtained results are essentially the same independent of the applied approach and they are given in Table I.

TABLE I. Comparison of the microscopic pK_a values of His290 and His291 sites in the OORO redox state of cytochrome oxidase at pH 7. The deprotonation energies are given in meV

His290	His291	Deprotonation energy	p$K_{a,7}$	Protonation state at pH 7
Titratable	Fixed-protonated	+170	9.8	Protonated
Titratable	Fixed-deprotonated	+590	16.9	Protonated
Fixed-protonated	Titratable	–140	4.7	Deprotonated
Fixed-deprotonated	Titratable	+295	12.0	Protonated

Results are shown only for the OORO redox state of CcO, since only then does deprotonation of His-ligand occur. According to previous work,[14] in the fully reduced (OORR) redox state of BNC, both histidines should be fully protonated with pK_a values well above 14.

It was found that His290 is protonated (pK_a 9.85) at pH 7 even if His291 is kept in the fixed protonated state, otherwise its p$K_{a,7}$ is 16.9. Interestingly, His291 site is also protonated (pK_a 12.0), if His290 is kept in the fixed deprotonated state. Obviously, double deprotonation of the ligated His sites would energetically destabilize the Cu_B center (It was found that the Cu_B complex in the CcO enzyme tries to preserve a total charge of +1). Using new updated pK_a values for the model-compounds does not change the essence that His291 wants to release a proton in the formally oxidized (OORO) redox state of the binuclear center (p$K_{a,7}$ 4.7) and in that sense, remains the potential proton-loading site.

*p*K$_a$ *Analysis of the Cu$_B$–His ligands*

To calculate the apparent pK_a values of the two His-ligands in CcO, they were considered as independent titratable groups without any restrictions, which could be simultaneously sampled. Their pK_a values were calculated in the self-consistent way, as the thermodynamic average over the charge states of all ionizable groups of CcO for a given redox state of the metal centers. The additivity of the solutions of the LPBE enables the breakdown the pK_a of the protonable group μ in protein (p$K_{a,\mu}^{protein}$) into four separate energy contributions: p$K_{a,\mu}^{model}$, the change in Born solvation energy, $\Delta\Delta G_\mu^{Born}$, interactions with background charges, $\Delta\Delta G_\mu^{back}$, and the energy of charge–charge interactions of titratable residues, $W_{\mu\nu}$.

The Born energy term arises from the interaction of the partial charges of the titratable group μ with its reaction field, which is mediated by the dielectric medium. This energy term, often referred to as the reaction field[34,41] or desolation penalty,[16] accounts for the change of the dielectric medium from aqueous solution to the inhomogeneous dielectric of the protein for the protonated and deprotonated form of the titratable group μ. The charged state is evidently much better solvated in the high dielectric of an aqueous solution and there is an energy penalty to transfer and solvate the titratable group inside the low dielectric of the protein. Moreover, the Born term describes the so-called reaction field,[48] while the sum of $\Delta\Delta G_\mu^{back}$ and $W_{\mu\nu}$ terms show the total effect of the protein charges on the titratable group μ, the so-called protein field.

In next step, the different energy contributions accounting for the apparent pK_a values in CcO were separated and analyzed, see Table II. The Born solvation term is directly related to desolvation penalty of ionization of the protonable site in low dielectric environment relative to the aqueous solvent. Therefore, the $\Delta\Delta G^{Born}_{HIS290}$ pushes up the pK_a of His290 by 6.6 p*K*-units. His291 is mostly located in a high dielectric cavity and the effect is opposite although much smaller. Quantum-mechanical charge transfer from Cu_B^{2+} to the His291 ligand, reflecting the charge distribution in the BNC, is the essential part responsible for the negative value of $\Delta\Delta G^{Born}_{HIS291}$.[45]

TABLE II. Breakdown of energy contributions to apparent pK_a values of His290 and His291 in OORO and OORR redox states of the enzyme at pH 7. For convenience, the energies are given in pK-units: 1 pK-unit = 59.5 meV = 1.37 kcal mol^{-1} = 5.74 kJ mol^{-1}

Redox state	Site	pK_a^{model} (1)	$\Delta\Delta G^{Born}$ (2)	$\Delta\Delta G^{back}$ (3)	p$K_a^{intrinsic}$ (1+2+3)	$W_{\mu v}$ (4)	Protein field (3+4)	p$K_a^{protein}$ (1+2+3+4)
OORO	His290	8.9	6.6	–3.3	12.2	4.7	1.4	16.9
	His291	8.9	–1.1	–15.5	–7.7	12.4	–3.1	4.7 (2.3[a])
	Δ	0	7.7	12.2	19.9	–7.7	4.5	12.2
OORR	His290	14.4	6.6	–0.7	20.3	5.4	4.7	25.7
	His291	14.4	–1.1	–11.4	1.9	14.1	2.7	16.0 (18.6[a])
	Δ	0	7.7	10.7	18.4	–8.7	2.0	9.7

[a]pK_a values of His291 computed using the default aqueous solution pK_a values of model compounds taken from the literature[14] for comparison

In the OORO redox state, $\Delta\Delta G_\mu^{back}$ energies of both His sites are downshifted. This is caused by the orientation of the backbone dipoles and the partial positive charges of the polar non-titratable residues and ionizable residues in their uncharged reference state. The background charges of the following residues interact particularly strongly with His291 causing a large downshift: polar – Trp126, Trp236, reference/neutral state of – Arg438, Arg439, all four propionates, Tyr129, and Tyr231. On other hand, the background charges of the neutral state of Asp364, PRAa_3, Tyr244, Tyr179 and Tyr304 act in favor of a small downshift of His290, as well as the H-bonding network including Thr309 and Phe305.

The intrinsic pK_a values of the two histidines would differ by ≈20 pK-units (12.2 *vs.* –7.7) if the whole enzyme would be in the neutral reference state of CcO. However, intrinsic pK_a values are only useful for theoretical constructions rather than measurable quantities.

The charge–charge interactions ($W_{\mu,v}$) with other ionizable sites create a pK_a increase of both His residues. This means that the effects of the negatively charged groups and residues dominate here; indeed at pH 7, the total calculated charge of CcO is –8. Once again, the effects are much stronger on the solvent-exposed His291 (12.4 *vs.* 4.7), since the charged titratable sites are mostly located in the hydrophilic area. Oppositely, the low dielectric inside the protein and membrane region favors the neutral protonation state of the titratable groups. If the effects of all four propionates (–4), Arg438(+) and Arg349(+) are summed up, the $W_{HIS291,v}$ upshift is 12.9 and the $W_{HIS290,v}$ upshift is 7.1 pK-units. The remaining difference comes from the other variably charged groups.

The magnitude of the reaction and protein field for His290 is +6.6 and +1.4, while for His291, they are –1.1 and –3.1 pK-units, respectively. Both reaction and protein field increase the pK_a of His290, but decrease the pK_a of His291 site, stabilizing the protonated state of one and the deprotonated state of the other His ligand of the Cu_B center in the OORO redox state of CcO.

For completeness, the results for the OORR redox state are also given in Table II. As expected, the corresponding Born energies remain the same in both oxidation states, if there is no redox-dependent conformational changes, *i.e.*, the dielectric boundaries remain the same. The entrance of an electron and the reduction of Cu_B center cause an increase in the $\Delta\Delta G_{\mu}^{back}$ energies of both His290/ /291 (2.6 *vs.* 4.1), as well as, a small increase in the $W_{\mu,v}$ charge–charge interaction energies (0.7 *vs.* 1.7). Consequently, both sites possess very high pK_a values in the OORR redox state of the protein – His290 (25.7) and His291 (16.0) being strongly protonated. The present study shows that the enhanced pK_a values of His291 site in the two redox states of CcO, obtained using the new pK_a values of the model compounds, are different from those given in a previous work,[14] but still fit very well within the proposed "His291 pumping model with kinetic gating".[28]

The stability of the obtained results may be questioned in respect to the used X-ray structure, since bovine CcO was solved in the fully reduced and fully oxidized redox state. Only rather small conformational changes, primarily localized in residue Asp51 and the region of heme *a*, have been reported in comparison of the fully reduced and fully oxidized crystal structures of bovine oxidase.[7,9] The root--mean square deviations around the binuclear center and the rest of the structure are a quite small, therefore, no significant divergences of the results in respect of this matter are expected. Furthermore, many different life forms, such as some bacteria, eukaryotic organisms, mammalian animals and humans, contain the aa_3-type of cytochrome *c* oxidase belonging to the so-called A-family. Recently, it was demonstrated that all species of the A-family show remarkable structural similarities of the two catalytic subunits, *A* and *B*. Moreover, their microscopic, electrostatic and thermodynamic properties of the key amino acid residues are almost identical, which strongly suggest a similar mechanism in a variety of different organisms.[25]

From molecular dynamics studies, it is known that transient conformational changes of the Glu242 side-chain[33] or Arg438/PRDa3 pair[14,29] are important for the proper function of CcO, but these changes cannot be observed by X-ray experiments. Nevertheless, the conformational gating could be relevant for the pumping mechanism in supplying and redirecting the protons to the PLS and BNC, or for preventing H^+ leak in the opposite direction. Cytochrome oxidase is a very complex and complicated enzyme system, which employs different control mechanisms and gating situations. Beside the kinetic gating mechanism, CcO also utilizes the conformational gating to ensure the unidirectionality of the proton translocation.

CONCLUSION

The focus of this work was to study the interactions of the dielectric and protein environment with the Cu_B center and its histidine ligands in cytochrome *c* oxidase. In the present work, continuum electrostatic calculations were employed to examine the influence of the protein environment on the pK_a values of His290 and His291 ligands of the Cu_B center for the different redox states of bovine CcO bound to the membrane. The magnitudes of the effects of the reaction and protein field on the pK_a values of the two histidine ligands of Cu_B center were evaluated. These histidines are mutually equivalent, with the same pK_a values in aqueous solution, but are quite different within the CcO enzyme. Their protonation energies, microscopic and apparent pK_a values were calculated and the breakdowns of the effects of the different energy contributions were analyzed to discover the source of their diverse behavior in the CcO enzyme. By using additivity of the solutions of the LPBE, the different energy contributions ($pK_{a,\mu}^{model}$, $\Delta\Delta G_\mu^{Born}$, $\Delta\Delta G_\mu^{back}$, $W_{\mu\nu}$) were separated and their effects on the acidity of the Cu_B histidine ligands discussed in light of the feasible proton-loading site and possible proton pumping mechanism in CcO.

The obtained microscopic and apparent pK_a values in the oxidized state of BNC were virtually the same, indicating that the deprotonated form of His291 accounts for the large pK_a increase of His290, since both the titratable sites on Cu_B center cannot be simultaneously in the charged state. It was concluded that only His291 exhibits redox-dependent protonation changes and therefore, may work as the PLS, while His290 prefers to stay in its protonated steady state in all redox states of the enzyme.

In addition, a new set of pK_a values in aqueous solution for the non-standard model compounds of the titratable sites within the binuclear complex, obtained by the DFT/solvation electrostatic calculations, were implemented. The new pK_a values of His291 in CcO are to some extent different from the results of previous studies,[14,30,31,49] but still compare well in respect to the protonation state. Thus, His291 is deprotonated with more reasonable pK_a value in the oxidized state of the BNC, while strongly protonated in the reduced state of CcO. His290 is in the protonated steady form in considered redox states. Therefore, the results of the present calculations support the proposed His291 model of the CcO pump. It is also remarkable that the local microenvironment around the Cu_B complex in CcO can generate such a huge difference (10–12 p*K*-units) in the acidity of the two coordinated histidines.

NOMENCLATURE

The following abbreviations are used: cyt *c*, cytochrome *c*; CcO, cytochrome *c* oxidase; LPBE, linear Poisson–Boltzmann Equation; PB, Poisson–Boltzmann; PRA*a*/PRD*a*, propionates A/D of heme *a*; PRAa_3/PRDa_3, propionates A/D of

heme a_3; PT, proton transfer; ET, electron transfer. Numeration of the residues corresponds to bovine CcO.

Acknowledgements. We gratefully acknowledge many helpful discussions with Prof. Alexei Stuchebrukhov from UC Davis. This work was financially supported by the Ministry of Education, Science and Technological Development of the Republic of Serbia: Grant No. 451-03-68/2020-14/200026 and Research Grant: OI 172035.

ИЗВОД

КАТАЛИТИЧКИ ЦЕНТАР ЦИТОХРОМ ОКСИДАЗЕ: УТИЦАЈ ПРОТЕИНСКОГ ОКРУЖЕЊА НА pK_a ВРЕДНОСТИ ХИСТИДИНСКИХ ЛИГАНАДА Cu_B ЦЕНТРА

ДРАГАН М. ПОПОВИЋ и ИВАНА С. ЂОРЂЕВИЋ

Универзитет у Београду - Институт за хемију, технологију и металургију, Центар за хемију – Институт од националног значаја за Републику Србију, Његошева 12, 11000 Београд

Молекулски механизам помоћу којег је пренос електрона спрегнут са протонском пумпом у цитохром с оксидази (CcO) представља један од главних нерешених проблема у биохемији. Посебно, природа и положај места везивања протона за пумпање (PLS) су главне тачке спорења. Cu_B комплекс има три хистидинска лиганда, при чему су само His290 и His291 титратибилни и међусобно слични са истим pK_a вредностима у воденом раствору, али су очигледно сасвим различити унутар CcO ензима. Раније је био предложен модел протонске пумпе у CcO са централном улогом His290, али недавни прорачуни наше групе показују да би His291, лиганд Cu_B центра, могао имати улогу PLS елемента, јер његово стање протоновања зависи од оксидационог стања бинуклеарног комплекса (BNC). Ова електростатичка студија примењена је за процену утицаја протеинског окружења на киселост два хистидина. Израчунали смо њихове pK_a вредности и раздвојили јачине ефеката различитих енергетских доприноса како бисмо открили природу њиховог различитог понашања у ензиму. Овде смо за нестандардна модел једињења унутар бинуклеарног комплекса користили нови сет са pK_a вредностима у воденом раствору. Побољшани резултати су упоређени са резултатима из претходних студија са бацањем акцента на могући механизам пумпања протона. Добијене микроскопске и макроскопске pK_a вредности у оксидованом стању BNC су практично исте, што индицира да депротоновани облик His291 изазива велики пораст pK_a вредности His290, јер оба титрациона места у Cu_B центру не могу истовремено бити у наелектрисаном стању. Приказани резултати подржавају предложени хистидински (His291) модел протонске пумпе.

(Примљено 20. јула, ревидирано 15. августа, прихваћено 20. августа 2020)

REFERENCES

1. M. Wikström, K. Krab, V. Sharma, *Chem. Rev.* **118** (2018) 2469 (https://doi.org/10.1021/acs.chemrev.7b00664)
2. J. P. Shapleigh, J. P. Hosler, M. M. J. Tecklenburg, Y. Kim, G. T. Babcock, R. B. Gennis, S. Ferguson-Miller, *Proc. Natl. Acad. Sci. USA* **89** (1992) 4786 (https://doi.org/10.1073/pnas.89.11.4786)
3. J. P. Hosler, S. Ferguson-Miller, D. A. Mills, *Ann. Rev. Biochem.* **75** (2006) 165 (https://doi.org/10.1146/annurev.biochem.75.062003.101730).
4. L. Qin, J. Liu, D. A. Mills, D. A. Proshlyakov, C. Hiser, S. Ferguson-Miller, *Biochemistry* **48** (2009) 5121 (https://doi.org/10.1021/bi9001387)

5. A. A. Konstantinov, S. Siletsky, D. Mitchell, A. Kaulen, R. B. Gennis, *Proc. Natl. Acad. Sci. USA* **94 (**1997) 9085 (https://doi.org/10.1073/pnas.94.17.9085).
6. A. K. L. Dürr, J. Koepke, P. Hellwig, H. Müller, H. Angerer, G. Peng, E. Olkhova, O. M. H. Richter, B. Ludwig, H. Michel, *J. Mol. Biol.* **384** (2008) 865 (https://doi.org/10.1016/j.jmb.2008.09.074)
7. S. Yoshikawa, K. Shinzawa-Itoh, R. Nakashima, R. Yaono, E. Yamashita, N. Inoue, M. Yao, M. J. Fei, C. P. Libeu, T. Mizushima, H. Yamaguchi, T. Tomizaki, T. Tsukihara, *Science* **280** (1998) 1723 (http://science.sciencemag.org/content/280/5370/1723)
8. A. M. Svensson-Ek, J. Abramson, G. Larsson, S. Tornroth, P. Brzezinski, S. Iwata, *J. Mol. Biol.* **321** (2002) 329 (https://doi.org/10.1016/S0022-2836(02)00619-8)
9. T. Tsukihara, K. Shimokata, Y. Katayama, H. Shimada, K. Muramoto, H. Aoyama, M. Mochizuki, K. Shinzawa-Itoh, E. Yamashita, M. Yao, Y. Ishimura, S. Yoshikawa, *Proc. Natl. Acad. Sci. USA* **100** (2003) 15304 (https://doi.org/10.1073/pnas.2635097100)
10. N. Yano, K. Muramoto, A. Shimada, S. Takemura, J. Baba, H. Fujisawa, M. Mochizuki, K. Shinzawa-Itoh, E. Yamashita, T. Tsukihara, S. Yoshikawa, *J. Biol. Chem*. **291** (2016) 23882 (https://www.jbc.org/content/291/46/23882)
11. H. Michel, *Proc. Natl. Acad. Sci. USA* **95** (1998) 12819 (https://doi.org/10.1073/pnas.95.22.12819)
12. T. K. Das, C. M. Gomes, M. Teixeira, D. L. Rousseau, *Proc. Natl. Acad. Sci. USA* **96** (1999) 9591 (ttps://doi.org/10.1073/pnas.96.17.9591).
13. M. Wikström, *Biochim. Biophys. Acta* **1458** (2000) 188 (https://doi.org/10.1016/S0005-2728(00)00068-2)
14. D. M. Popovic, A. A. Stuchebrukhov, *J. Am. Chem. Soc.* **126** (2004) 1858 (https://doi.org/10.1021/ja038267w)
15. K. Faxen, G. Gilderson, P. Ädelroth, P. Brzezinski, *Nature* **437** (2005) 286 (https://doi.org/10.1038/nature03921)
16. Y. Song, E. Michonova-Alexova, M. R. Gunner, *Biochemistry* **45** (2006) 7959 (https://doi.org/10.1021/bi052183d)
17. M. A. Sharpe, S. Ferguson-Miller, *J. Bioenerg. Biomembr.* **40** (2008) 541 (https://doi.org/10.1007/s10863-008-9182-6).
18. J. A. Fee, D. A. Case, L. Noodleman, *J. Am. Chem. Soc.* **130** (2008) 15002 (https://doi.org/10.1021/ja803112w)
19. S. A. Siletsky, A. A. Konstantinov, *Biochim. Biophys. Acta* **1817** (2012) 476 (https://doi.org/10.1016/j.bbabio.2011.08.003)
20. I. Belevich, D. A. Bloch, N. Belevich, M. Wikström, M. I. Verkhovsky, *Proc. Natl. Acad. Sci. USA* **104** (2007) 2685 (https://doi.org/10.1073/pnas.0608794104)
21. S. Han, S. Takahashi, D. L. Rousseau, *J. Biol. Chem.* **275** (2000) 1910 (https://doi.org/10.1074/jbc.275.3.1910)
22. M. Wikström, *Biochim. Biophys. Acta* **1655** (2004) 241 (https://doi.org/10.1016/j.bbabio.2003.07.013)
23. P. Brzezinski, R. B. Gennis, *J. Bioenergy Biomembr.* **40** (2008) 521 (https://doi.org/10.1007/s10863-008-9181-7)
24. C. M. Soares, A. M. Baptista, M. M. Pereira, M. Teixeira, *J. Biol. Inorg. Chem.* **9** (2004) 124 (https://doi.org/10.1007/s00775-003-0509-9)
25. D. M. Popovic, I. V. Leontyev, D. G. Beech, A. A. Stuchebrukhov, *Proteins Struct. Funct. Bioinform.* **78** (2010) 2691 (https://doi.org/10.1002/prot.22783)
26. D. M. Popovic, *Amino Acids* **45** (2013) 1073 (https://doi.org/10.1007/s00726-013-1585-y)

27. W.-G. Han Du, A. W. Götz, L. Noodleman, *Inorg. Chem*. **57** (2018) 1048 (https://doi.org/10.1021/acs.inorgchem.7b02461)
28. D. M. Popovic, A. A. Stuchebrukhov, *FEBS Letters* **566** (2004) 126 (https://doi.org/10.1016/j.febslet.2004.04.016)
29. D. M. Popovic, A. A. Stuchebrukhov, *J. Phys. Chem., B* **109** (2005) 1999 (https://doi.org/10.1021/jp0464371)
30. D. M. Popovic, J. Quenneville, A. A. Stuchebrukhov, *J. Phys. Chem., B* **109** (2005) 3616 (https://doi.org/10.1021/jp046535m)
31. J. Quenneville, D. M. Popovic, A. A. Stuchebrukhov, *Biochim. Biophys. Acta* **1757** (2006) 1035 (https://doi.org/10.1016/j.bbabio.2005.12.003)
32. D. M. Popovic, A. A. Stuchebrukhov, *Biochim. Biophys. Acta* **1817** (2012) 506 (https://doi.org/10.1016/j.bbabio.2011.10.013)
33. D. M. Popovic, A. A. Stuchebrukhov, *Photochem. Photobiol. Sci.* **5** (2006) 611 (https://doi.org/10.1039/B600096G)
34. D. Bashford, K. Gerwert, *J. Mol. Biol*. **224** (1992) 473 (https://doi.org/10.1016/0022-2836(92)91009-E)
35. D. Bashford, *Scientific Computing in Object-Oriented Parallel Environments*, Springer, Berlin, 1997, p. 233 (https://www.springer.com/gp/book/9783540638278)
36. M. R. Gunner, B. Honig, *Proc. Natl. Acad. Sci. USA* **88** (1991) 9151 (https://doi.org/10.1073/pnas.88.20.9151)
37. A.-S. Yang, M. R. Gunner, R. Sompogna, B. Honig, *Prot. Struct. Funct. Gen.* **15** (1993) 252 (https://doi.org/10.1002/prot.340150304)
38. D. Bashford, D. A. Case, C. Dalvit, L. Tennant, P. E. Wright, *Biochemistry* **32** (1993) 8045 (https://doi.org/10.1021/bi00082a027)
39. P. Beroza, D. R. Fredkin, *J. Comput. Chem.* **17** (1996) 1229 (https://doi.org/10.1002/(SICI)1096-987X(19960730)17:10<1229::AID-JCC4>3.0.CO;2-Q)
40. J. Antosiewicz, J. M. Briggs, A. H. Elcock, M. K. Gilson, J. A. McCammon, *J. Comput. Chem.* **17** (1996) 1633 (https://doi.org/10.1002/(SICI)1096-987X(19961115)17:14<1633::AID-JCC5>3.0.CO;2-M)
41. J. Li, M. R. Nelson, C. Y. Peng, D. Bashford, L.Noodleman, *J. Phys. Chem., A* **102** (1998) 6311 (https://doi.org/10.1021/jp980753w)
42. A. Warshel, A. Papazyan, *Curr. Opin. Struct. Biol.* **8** (1998) 211 (https://doi.org/10.1016/S0959-440X(98)80041-9)
43. P. J. Martel, C. M. Soares, A. M. Baptista, M. Fuxreiter, G. Naray-Szabo, R. O. Louro, M. A. Carrondo, *J. Biol. Inorg. Chem.* **4** (1999) 73 (https://doi.org/10.1007/s007750050291)
44. D. M. Popovic, A. Zmiric, S. D. Zaric, E. W. Knapp, *J. Am. Chem. Soc.* **124** (2002) 3775 (https://doi.org/10.1021/ja016249d)
45. J. Quenneville, D. M. Popovic, A. A. Stuchebrukhov, *J. Phys. Chem., B* **108** (2004) 18383 (https://doi.org/10.1021/jp0467797)
46. D. M. Popovic, S. D. Zaric, B. Rabenstein, E. W. Knapp, *J. Am. Chem. Soc.* **123** (2001) 6040 (https://doi.org/10.1021/ja003878z)
47. V. Couch, D. Popovic, A. A. Stuchebrukhov, *Biophys. J.* **101** (2011) 431 (https://doi.org/10.1016/j.bpj.2011.05.068)
48. D. S. Cerutti, N. A. Baker, J. A. McCammon, *J. Chem. Phys.* **127** (2007) 155101 (https://doi.org/10.1063/1.2771171)
49. D. V. Makhov, D. M. Popovic, A. A. Stuchebrukhov, *J. Phys. Chem., B* **110** (2006) 12162 (https://doi.org/10.1021/jp0608630).